ChemComm

Photoinduced charge flow inside an iron porphyrazine complex

Journal:	*ChemComm*
Manuscript ID	CC-COM-08-2019-006193.R1
Article Type:	Communication

COMMUNICATION

Photoinduced charge flow inside an iron porphyrazine complex

Longteng Tang,[a] Liangdong Zhu,[a] Maraia E. Ener,[b,‡] Hongxin Gao,[c,§] Yanli Wang,[a] John T. Groves,[c] Thomas G. Spiro*[b] and Chong Fang*[a]

Received 00th January 20xx,
Accepted 00th January 20xx

DOI: 10.1039/x0xx00000x

Tracking inorganic photochemistry with high resolution poses considerable challenges. Here, sub-picosecond electronic and structural motions and MLCT/d-d intersystem crossing in a cationic iron-porphyrazine are probed using ultrafast transient absorption, stimulated Raman spectroscopy, and quantum calculations. By delineating photoinduced energy relaxation, strategies for extending the lifetime of MLCT state are discussed.

Porphyrazines (Pz's) and metalloporphyrazines (MPz's) are tetrapyrrole macrocyclic compounds that belong to the porphyrinoid family.[1] Due to their versatile optical and chemical properties, they have been used as sensitizers in photodynamic therapy (PDT), molecular scaffolds in nanoarchitectures, and catalysts in redox reactions.[1c,2] Recently, Gao and Groves reported a novel hydroxoferric porphyrazine complex with fused pyridinium groups (Fig. 1A inset), $[(PyPz)Fe^{III}(OH)(OH_2)]^{4+}$, which can cleave moderately strong C–H bonds via hydrogen atom transfer (HAT).[3] The reaction rate is orders of magnitude faster than other reported ferric complexes and faster than typical ferryl species. The product complex, $[(PyPz)Fe^{II}(OH_2)_2]^{4+}$ (which we abbreviate to FePz, see ESI† for the detailed synthesis methods), could be a photocatalyst. This is because a metal-to-ligand charge transfer (MLCT) transition of the photoexcited FePz, which might be stabilized by the positive charges on the ligand ring system, would formally oxidize Fe^{II} to Fe^{III}. If the MLCT state lived long enough to be quenched by an electron acceptor or an electrode, permitting deprotonation of Fe^{III}–OH_2, then the substrates could be hydroxylated photocatalytically.

Regardless of the photocatalytic potential, iron complexes typically have very short excited state lifetimes. Accordingly, deciphering the correlated electronic and atomic motions of these complexes, which could govern their functionality, is of crucial importance. Here, we have investigated the primary events following FePz photoexcitation using both transient absorption (TA) spectroscopy and tunable femtosecond stimulated Raman spectroscopy (FSRS) spectroscopy to track the excited state electronic and structural evolution in real time.[4] Detailed spectroscopic methods can be found in the ESI†. FSRS is a powerful technique to capture transient vibrational modes in the ground and excited states. Recent applications include the spin-crossover dynamics in an Fe^{II} complex,[5] energy redistribution in the excited state heme of myoglobin,[6] and excited state dynamics in a Ni^{II} phthalocyanine (Pc) complex.[4c]

The FePz absorption spectrum in aqueous buffer solution (Fig. 1A) shows the classical porphyrinoid Q and B bands at ~633 and 354 nm, and also a moderately strong band at ~480 nm that is absent in the absorption spectrum of the ferric complex.[3] This band is assigned to the anticipated MLCT transition (Fig. 1), also allowing us to optimize ultrafast laser excitation wavelengths in

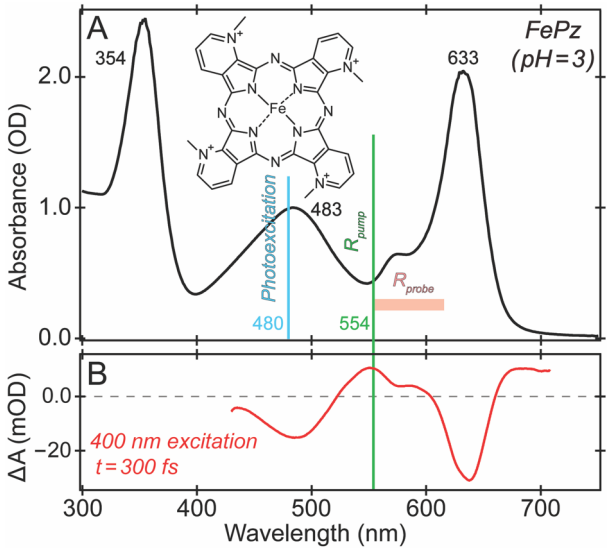

Fig. 1 Ground and excited state electronic spectra of the FePz complex. (A) Steady-state absorption spectrum of FePz in pH=3 buffer. Chemical structure is shown in the inset. (B) Transient absorption of FePz at 300 fs following 400 nm excitation. The actinic pump, Raman pump and probe wavelengths are marked.

[a] Department of Chemistry, Oregon State University, 153 Gilbert Hall, Corvallis, Oregon 97331, United States. E-Mail: Chong.Fang@oregonstate.edu
[b] Department of Chemistry, University of Washington, Seattle, Washington 98195, United States. E-Mail: spirot@uw.edu
[c] Department of Chemistry, Princeton University, Princeton, New Jersey 08544, United States
[‡] Present address: Department of Chemistry, Yale University, 225 Prospect St., New Haven, Connecticut 06511, United States.
[§] Present address: Procter & Gamble Technology (Beijing) Co., Ltd., No. 35 Yu'an Road, Shunyi District, Beijing 101312, P. R. China.

†Electronic Supplementary Information (ESI) available: Details of the experimental materials and spectroscopic methods, Fig. S1-S5 on additional TA and FSRS analysis, Tables S1-S2 on quantum calculation results. See DOI: 10.1039/x0xx00000x

a tunable FSRS optical setup. The two pK_a values of FePz were measured to be 8.0 and 10.1, so at pH=3 the two axial water ligands remain protonated (see ESI† text for more details).[3,7]

Femtosecond (fs)-TA spectra were collected to characterize the excited electronic states (Fig. 1B and Fig. S1, ESI†); the main features were found to be independent of the excitation wavelength, consistent with a common de-excitation pathway. A representative difference spectrum (Fig. 1B) shows two ground-state (GS) bleaching bands centered at 485 and 635 nm, and two excited state (ES) absorption bands at 550 nm and around 700 nm. They all decay with a ~4 ps lifetime (Fig. S1-S3), establishing a rapid ground state recovery.[8] The ~700 nm band emerges within the cross-correlation time (<100 fs) and shifts to the blue as it decays (Fig. S2), while the 550 nm band has a delayed rise (~230 fs, Fig. S3) and also shifts to the blue side.

The FSRS spectra were recorded after photoexcitation at 480 nm, into the MLCT band. The Raman pump wavelength was strategically tuned to 554 nm in order to minimize absorption by the ground state, and to exploit resonance with the ~550 nm ES band (Fig. 1). No clear ES Raman spectrum was observed at other wavelength combinations, substantiating the importance of optimizing FSRS signal strength guided by TA spectroscopy with knowledge about excited state energetics (ESI†). Despite the almost continuous electronic absorption bands across the near-UV to near-IR region (Fig. 1A), this experimental approach with a close-knit feedback loop ensures the optimal FSRS signal-to-noise ratio.[4e,4f] Therefore, crucial structural dynamics insights along the multidimensional photochemical reaction coordinates of FePz in water can be obtained. Fig. 2 presents the time-resolved 2D contour plot of the Stokes (red-side) Raman spectrum from –300 fs to 1.5 ps to highlight the ultrafast process (see an expanded plot from –300 fs to 40 ps in Fig. S4).

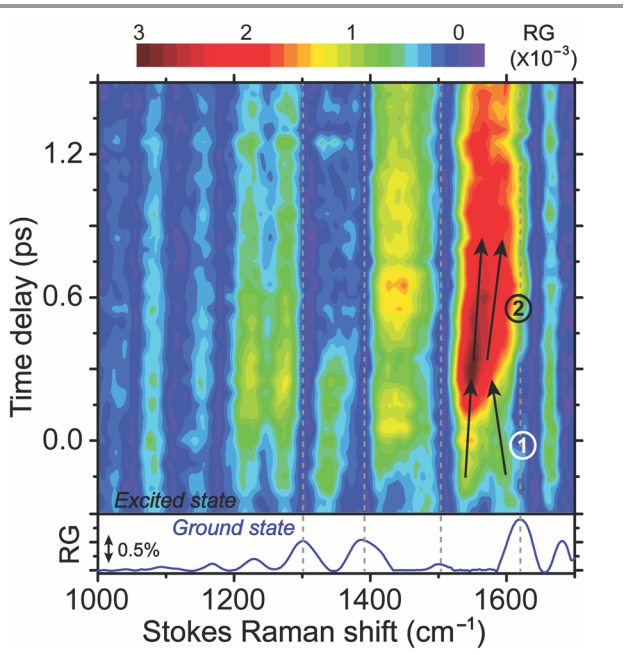

Fig. 2 Contour plot of the time-resolved ES-FSRS spectra from –300 fs to 1.5 ps after 480 nm photoexcitation of FePz. Raman pump was tuned to 554 nm with a redder Raman probe. The ground state spectrum is plotted at the bottom. The vertical gray lines highlight the vibrational frequency change from the GS to ES.

The ES Raman modes exhibit instantaneous frequency shifts from the GS peak positions (see the GS Raman spectrum at the bottom of Fig. 2). In particular, the ~1505 and 1620 cm^{-1} GS modes (marked by vertical dashed lines in Fig. 2) exhibit large shifts to ~1550 and 1595 cm^{-1} in the ES, respectively, reflecting substantial charge redistribution from GS to the transient MLCT state.[9] Subsequent frequency shifts on the fs to ps timescale track structural changes in and out of this MLCT state, implying that these vibrational motions could be actively promoting charge transfer instead of being some passive spectator modes. This is because electron motions, of themselves, should enable the electronic transitions on a much shorter timescale.[4d,4f]

Normal mode calculations were carried out on FePz, including the axial water molecules, with density functional theory (DFT) at the RB3LYP/6-31G level using Gaussian 09 (see Table S1 for details about the mode frequencies from quantum calculations and vibrational assignment).[10] We then performed time-dependent DFT (TD-DFT) at the same level, and also with genecp basis sets (SDD or Lanl2dz for Fe, 6-31G(d,p) for C, H, O, N; see Table S2). The usual frequency scaling factor of 0.96 was employed.[11] Atomic motions of the vibrational modes falling closest to 1550 and 1595 cm^{-1} are shown in Fig. 3B and C. The former mode involves mostly stretching of the inner ring C=N bonds, while the latter has mostly C=C and C=N contributions from the outer ring (i.e., methylpyridinium modes, see Table S1 in ESI† for pertinent nuclear motions of strong Raman bands).

The clear up and down-shifts experienced by these two characteristic modes (i.e., 1505→1550 cm^{-1} and 1620→1595 cm^{-1}) from $S_0 \rightarrow S_1$ are attributable to the photoinduced MLCT transition. Electron transfer from Fe^{II} to the Pz conjugated π system is expected to weaken the outer ring bonds (electric charge is transferred to a π^* orbital), while the increase in Fe positive charge (see ESI† text, and Table S2 for the calculated charges on the central metal) should strengthen the Fe–N bonds and contract the inner ring (i.e., Fe^{III} is smaller and has shorter metal-ligand bonds than Fe^{II}). Notably, the inner ring mode is similar to the ν_{10} mode of porphyrins, which is known to increase in frequency with a decreasing "core" size.[4c] The formal electric charge characterization is an exaggeration, since the Fe and Pz orbitals are highly mixed. Also, there could be a Jahn-Teller effect in the electronic excited state that changes bond distances in the ligand ring system. Nevertheless, our various DFT and TD-DFT calculations confirm an increase in the excited state Fe positive charge (Table S2), consistent with the MLCT assignment upon actinic photoexcitation of FePz in water.

For both Raman marker bands, these notable instantaneous frequency shifts are followed by continuing shifts in the same direction during the first 0.4 ps (Fig. 3A), reflecting evolution of the MLCT state to its minimum energy structure. At this point the outer ring stretch shifts back up, while the inner ring stretch, after a pause, continues to shift up. We attribute this new phase to a transition from the MLCT state to an adjacent d-d state. The reversal of the outer ring shift reflects back electron transfer from Pz to Fe. In an earlier FSRS study of an Fe(II)-Schiff base complex,[5] a similar upshift of a ligand ring C=N stretching mode at 1650 cm^{-1} signaled spin-conversion to a d-d state; the relaxation time was ~190 fs, similar to our observation (Fig. 3A,

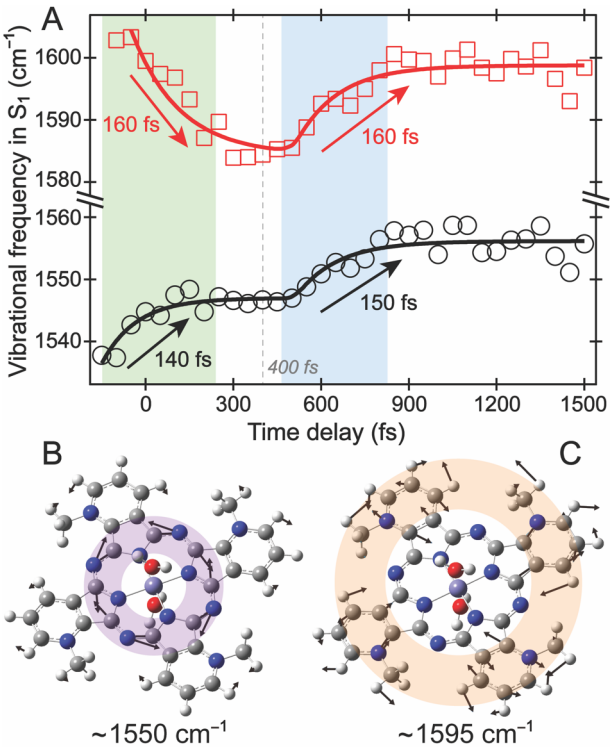

Fig. 3 Excited-state vibrational frequency dynamics of two high-frequency marker bands of FePz in aqueous solution. (A) Frequency shifts of the ca. 1550 (black) and 1595 cm^{-1} (red) modes are least-squares fitted with the exponential time constants denoted. Pertinent atomic motions from quantum calculations are shown in (B) and (C) with detailed mode assignments presented in Table S1 (ESI†). The inner and outer ligand rings are highlighted by the violet and orange ring shades, respectively.

cyan shade). The intermediate temporal region (between two shaded areas, Fig. 3A) implies that the two ultrafast CT processes are stepwise and involve electron motions in the opposite directions (see Scheme 1 and TOC Graphic). Notably, the signal-to-noise ratio of the observed Raman modes (Fig. 2) is intimately related to resonance conditions as the system navigates the excited-state potential energy surface, which rationalizes the apparent delayed onset of some vibrational marker bands (e.g., the ~1550 and 1595 cm^{-1} modes) with their peak intensity maxima appearing after the photoexcitation time zero. The least-squares fitting of multiple exponential functions thus need to empirically address this effect by slightly shifting the fitted time zero to uncover more accurate time constants associated with transitions between transient electronic states, which achieve dynamic resonance enhancement[4f,12] for the observed Raman marker bands in the electronic excited state (e.g., Fig. 4 and Fig. S5 with further discussions in ESI†).

The back electron transfer does not return the complex to the S=0 ground state, and so must be to one of the higher-lying d orbitals: $d_{x^2-y^2}$ or d_{z^2}. The latter would be lower in energy since the axial water molecules are weaker ligands than the in-plane pyrrole N atoms. An electron in the d_{z^2} orbital would weaken the Fe–OH_2 bonds, relieving their non-bonded contacts with the pyrrole N atoms, and allowing the Pz ring to contract further, thus accounting for the continuing upshift of the inner ring stretch (black trace in Fig. 3A). The $d_{x^2-y^2}$ orbital remains unoccupied, requiring an intermediate-spin (triplet) state with unpaired electrons in the d_{z^2} and a $d\pi$ orbital.

This interpretation of the FSRS data is supported by the TA temporal profiles (Fig. S3 and S5, ESI†). The intensity of the ES 680 nm band rises within the cross-correlation time, but the 550 nm band is delayed, arising in concert with the FSRS mode intensity, both reaching a maximum at ~0.4 ps (Fig. 4), when the FSRS frequency shifts (Fig. 3A) indicate the transition to the d-d state. The 550 nm TA band can be mainly attributed to this state, its intensity providing the crucial dynamic resonance enhancement for the observed ES-FSRS signal.[4f] Due to the conjugated ligand ring system, delayed peak intensities of several high-frequency Raman modes above 1200 cm^{-1} can be seen in Fig. 2, supporting the retrieved time constants in Fig. 3A and Fig. S5 (ESI†) with ultrafast Raman peak frequency and intensity dynamics. Beyond 0.4 ps, the TA and FSRS intensities both decay in two phases with time constants of ca. 0.3 and 3–4 ps. The former process likely reflects vibrational relaxation within the metal-centered d-d state, while the latter tracks ground state recovery including vibrational cooling therein.[13]

The inferred photocycle is illustrated in Scheme 1. Excitation to the MLCT state is followed by relaxation (0.15 ps) from the Franck-Condon region, and then intersystem crossing (0.16 ps) to the d-d state, which relaxes (0.3 ps) and decays to the ground state (4 ps). This reaction sequence differs significantly from that observed recently for a Ni^{II} phthalocyanine complex $NiPc(OBu)_8$, wherein excitation to the π-π* states was followed by rapid intersystem crossing first to a d-d state, and then to a longer-lived (500 ps) ligand-metal charge transfer (LMCT) state.[4c] This state was enabled by the electron-donating butoxy substituents on the Pc macrocycle, while in our current work, the electron-withdrawing N-methylpyridinium substituents on the porphyrazine ring produce a low-lying MLCT state. The MLCT energy, however, remains above that of the d-d state (Scheme 1). Another notable difference is that in $NiPc(OBu)_8$ the macrocycle is expanded, not contracted, in the d-d state, indicating that electrons occupy both the d_{z^2} and $d_{x^2-y^2}$ orbitals. It is possible that that the $d_{x^2-y^2}$ orbital remains

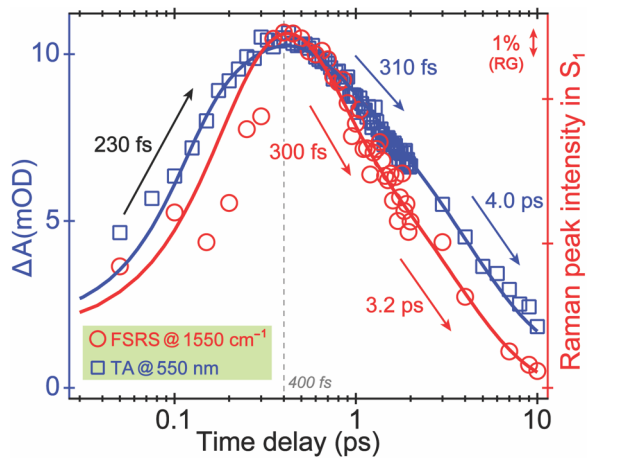

Fig. 4 Correlated fs-TA and FSRS dynamics on ultrafast reaction timescales. The ES band at 550 nm (blue, left axis) and the 1550 cm^{-1} mode (red, right axis) exhibit similar rise and decay dynamics. The fits (solid curves) with time constants and the Raman gain (RG) magnitude are shown within a 10 ps time window.

Scheme 1 Photoinduced charge flow inside the novel FePz complex in aqueous solution: an ultrafast reaction unveiled by fs-TA and tunable FSRS

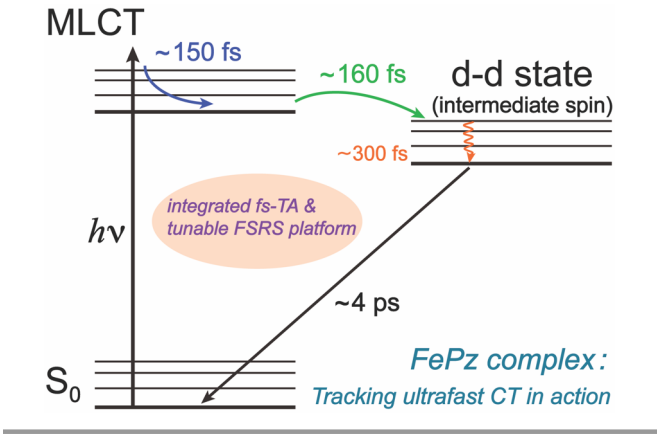

unoccupied in FePz (this work) because the Fe^{II}–Pz bonds are stronger than the Ni^{II}–Pc bonds, owing to the Fe^{II}–Pz back donation.[14] The strength of the Pz ligand field is evidenced by the bis-aqua complex being low-spin (sharp line NMR)[3] despite water being a weak field ligand. In fact, Pz has been shown to have a stronger field than either porphyrin or Pc.[14]

In any event, the elucidated FePz orbital energy ordering leads to rapid deactivation of the MLCT state, and thus, a short-lived excited state. It is likely, however, that the photocatalytic potential of FePz could be rationally realized through molecular engineering. The MLCT/d-d intersystem crossing results from back electron-transfer to the d_{z^2} orbital of the central metal, whose energy depends on the axial ligand field. If one of the axial water molecules were replaced by a strong field ligand, the d-d state might be pushed above the MLCT state, which could consequently live long enough to support photocatalysis.[8a,15] Further studies are planned to exploit this strategy, aided by our spectroscopy platform. Encouragingly, $[(TMPyP)Co^{III}(OH_2)_2]^{5+}$ was reported to have a much longer lived (~100 μs) triplet excited state.[16] This Co^{III} complex is isoelectronic with FePz but has a higher ligand field, reflected in a decreased first pK_a of the water ligand (~6, versus 8 for FePz)[7,17] and thus a larger d-d gap.

In summary, with strategic tuning of photoexcitation and Raman pump wavelengths, a synergistic use of fs-TA, DFT calculations, and excited-state FSRS allows us to delineate the ultrafast charge transfer and structural events inside a novel iron porphyrazine complex with highly correlated electronic and vibrational motions. Frequency dynamics of key Raman modes reveal excited state structural motions of FePz involving the inner and outer Pz rings. The initial MLCT state undergoes rapid relaxation (150 fs), which efficiently transitions (160 fs) into an energetically adjacent d-d state before returning to the ground state. These findings offer essential insights into developing novel functional metal-organic complexes (especially with the earth-abundant metals such as iron) in broad applications from redox reactions, photosynthesis to dye-sensitized solar cells.

This work was funded by the NSF CAREER Grant (CHE-1455353 to C.F.) and NIH (2R37 GM036298 to J.T.G). M.E.E. was supported by the Irving S. Sigal Postdoctoral Fellowship (ACS). The authors thank Prof. Cody Schlenker (University of Washington, Washington Research Foundation) for access to the TA laser system. We also thank Dr. Alexandra Soldatova for helpful discussions.

Conflicts of interest

There are no conflicts to declare.

Notes and references

1 (*a*) M. S. Rodríguez-Morgade and P. A. Stuzhin, *J. Porphyr. Phthalocya.*, 2004, **8**, 1129-1165; (*b*) B. Szyszko, M. J. Białek, E. Pacholska-Dudziak and L. Latos-Grażyński, *Chem. Rev.*, 2017, **117**, 2839-2909; (*c*) X. Huang and J. T. Groves, *Chem. Rev.*, 2018, **118**, 2491-2553.

2 (*a*) M. Zhao, C. Stern, A. G. M. Barrett and B. M. Hoffman, *Angew. Chem. Int. Ed.*, 2003, **42**, 462-465; (*b*) K. F. Cheng, N. A. Thai, L. C. Teague, K. Grohmann and C. M. Drain, *Chem. Commun.*, 2005, 4678-4680; (*c*) S. Ristori, A. Salvati, G. Martini, O. Spalla, D. Pietrangeli, A. Rosa and G. Ricciardi, *J. Am. Chem. Soc.*, 2007, **129**, 2728-2729; (*d*) T. P. Umile, D. Wang and J. T. Groves, *Inorg. Chem.*, 2011, **50**, 10353-10362; (*e*) V. Engelhardt, S. Kuhri, J. Fleischhauer, M. García-Iglesias, D. González-Rodríguez, G. Bottari, T. Torres, D. M. Guldi and R. Faust, *Chem. Sci.*, 2013, **4**, 3888-3893; (*f*) J. Piskorz, K. Konopka, N. Düzgüneş, Z. Gdaniec, J. Mielcarek and T. Goslinski, *ChemMedChem.*, 2014, **9**, 1775-1782.

3 H. Gao and J. T. Groves, *J. Am. Chem. Soc.*, 2017, **139**, 3938-3941.

4 (*a*) P. Kukura, D. W. McCamant and R. A. Mathies, *Annu. Rev. Phys. Chem.*, 2007, **58**, 461-488; (*b*) C. Fang, R. R. Frontiera, R. Tran and R. A. Mathies, *Nature*, 2009, **462**, 200-204; (*c*) G. Balakrishnan, A. V. Soldatova, P. J. Reid and T. G. Spiro, *J. Am. Chem. Soc.*, 2014, **136**, 8746-8754; (*d*) D. R. Dietze and R. A. Mathies, *ChemPhysChem*, 2016, **17**, 1224–1251; (*e*) W. Liu, Y. Wang, L. Tang, B. G. Oscar, L. Zhu and C. Fang, *Chem. Sci.*, 2016, **7**, 5484-5494; (*f*) C. Fang, L. Tang, B. G. Oscar and C. Chen, *J. Phys. Chem. Lett.*, 2018, **9**, 3253-3263.

5 A. L. Smeigh, M. Creelman, R. A. Mathies and J. K. McCusker, *J. Am. Chem. Soc.*, 2008, **130**, 14105-14107.

6 C. Ferrante, E. Pontecorvo, G. Cerullo, M. H. Vos and T. Scopigno, *Nat. Chem.*, 2016, **8**, 1137-1143.

7 R. Gilson and M. C. Durrant, *Dalton Trans.*, 2009, 10223-10230.

8 (*a*) L. Liu, T. Duchanois, T. Etienne, A. Monari, M. Beley, X. Assfeld, S. Haacke and P. C. Gros, *Phys. Chem. Chem. Phys.*, 2016, **18**, 12550-12556; (*b*) S. G. Shepard, S. M. Fatur, A. K. Rappé and N. H. Damrauer, *J. Am. Chem. Soc.*, 2016, **138**, 2949-2952.

9 R. A. Reed, R. Purrello, K. Prendergast and T. G. Spiro, *J. Phys. Chem.*, 1991, **95**, 9720-9727.

10 M. J. Frisch, et al., *Gaussian 09, Revision B.1,* Gaussian, Inc., Wallingford, CT, 2009.

11 E. J. Baerends, G. Ricciardi, A. Rosa and S. J. A. van Gisbergen, *Coord. Chem. Rev.*, 2002, **230**, 5-27.

12 (*a*) W. Liu, L. Tang, B. G. Oscar, Y. Wang, C. Chen and C. Fang, *J. Phys. Chem. Lett.*, 2017, **8**, 997–1003; (*b*) B. G. Oscar, C. Chen, W. Liu, L. Zhu and C. Fang, *J. Phys. Chem. A*, 2017, **121**, 5428-5441.

13 S. Franzen, L. Kiger, C. Poyart and J.-L. Martin, *Biophys. J.*, 2001, **80**, 2372-2385.

14 M.-S. Liao, J. D. Watts and M.-J. Huang, *J. Phys. Chem. A*, 2005, **109**, 7988-8000.

15 P. Chábera, Y. Liu, O. Prakash, E. Thyrhaug, A. E. Nahhas, A. Honarfar, S. Essén, L. A. Fredin, T. C. B. Harlang, K. S. Kjær, K. Handrup, et al., *Nature*, 2017, **543**, 695-699.

16 M. A. Fodor, O. Horváth, L. Fodor, G. Grampp and A. Wankmüller, *Inorg. Chem. Commun.*, 2014, **50**, 110-112.

17 R. J. H. Chan, Y. O. Su and T. Kuwana, *Inorg. Chem.*, 1985, **24**, 3777-3784.

Sub-picosecond electronic and structural motions and MLCT/d-d intersystem crossing in an iron-porphyrazine are revealed using transient absorption and femtosecond stimulated-Raman spectroscopy.

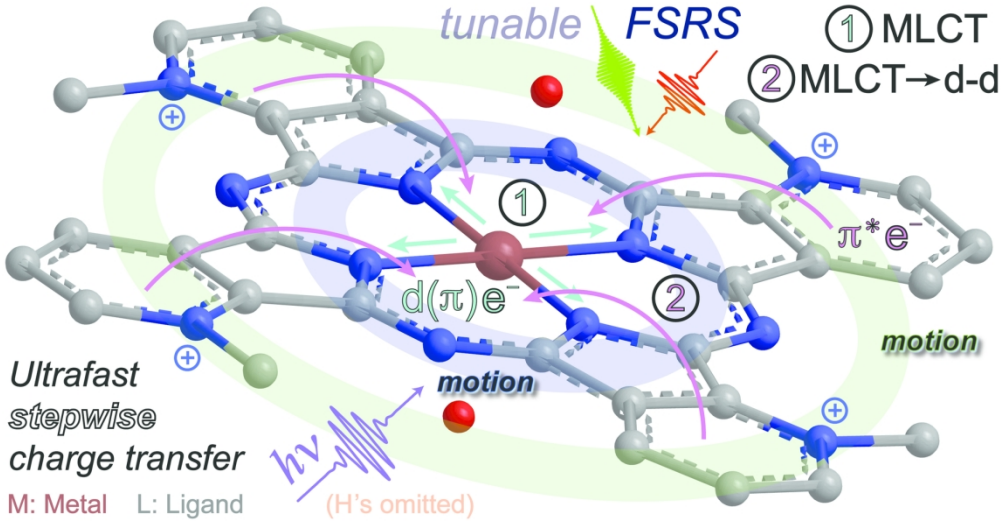

81x42mm (600 x 600 DPI)